Bidirectional wavelength tuning of individual semiconductor quantum dots in a flexible rolled-up microtube

S. Mendach,* S. Kiravittaya, A. Rastelli,† M. Benyoucef,† R. Songmuang,‡ and O. G. Schmidt†
Max-Planck-Institut für Festkörperforschung, Heisenbergstraße 1, D-70569 Stuttgart, Germany
(Received 13 May 2007; published 18 July 2008)

We consider a pair of artificial atoms with different ground-state energies. By means of finite element calculations, we predict that the ground-state energies can be tuned into resonance if the artificial atoms are placed into a flexible ring structure, which is elastically deformed by an external force. This concept is experimentally verified by embedding self-assembled quantum dots with low density into the wall of a rolled-up microtube ring resonator. We demonstrate that quantum dots can elastically be tuned in and out of resonance with each other or with the ring resonator modes.

DOI: 10.1103/PhysRevB.78.035317 PACS number(s): 78.66.Fd, 42.55.Sa, 46.70.−p, 78.67.Hc

A wide and accurate control over physical parameters in semiconductors is unique and has caused the great success of semiconductor physics and technology in the past. Semiconductor quantum dots (QDs) lie at the heart of many exciting devices and physical concepts, e.g., single-photon sources, qubits, and entangled photons.[1–3] A key task for almost all applications envisioned is a deterministic control over the emission energy of individual QDs. Irreversible tuning techniques such as post-growth rapid thermal annealing[4] might be used to tune the QD emission into the desired emission energy range. More recently, it has been shown that *in situ* laser processing[5] can be used to accurately blueshift emission lines of individual QDs. However, reversible tuning might be required for further adjustment of the energies and for refined single-quantum dot on-chip applications. Global reversible tuning with external magnetic field,[6] temperature,[7,8] or uniaxial stress[9] is not suitable to individually address close-by QDs. Recent experiments[10] suggest that electric-field induced Stark shifts in vertical quantum dot molecules[11] might be used to achieve resonance of two QDs in a resonator.

Here we propose to use local stress as a reversible tuning parameter for the emission energies of individual QDs. Individual QDs are addressed differently due to the inhomogeneous strain distribution induced in the sample. The desired energetic QD shifts can be obtained by creating the corresponding strain distribution. As an example, we consider two QDs, which are embedded into the wall of a flexible microtube optical ring resonator. Our calculations predict that upon local deformation of the ring resonator, reversible spectral shifts into the red and blue of several tens of millielectron volt can be achieved for the two QDs. Depending on the relative position and magnitude of the applied force, the two QDs can be tuned into mutual resonance and into resonance with the optical mode. Experimentally, we verify this concept for In(Ga)As QDs with low density embedded in the wall of a rolled-up microtube ring resonator.[12–17] Energy shifts as large as 20 meV are achieved for the QDs, and optical coincidence between two QDs as well as a QD and the ring resonator mode are demonstrated.

Figure 1 shows a point force applied to the top of an optical microtube ring resonator. Based on the finite element method (FEM), a numerical calculation is performed to quantitatively describe the tube deformation and the strain induced energy shifts of two QDs located in the wall of the deformed tube.[18] For our calculations we approximate the flexible ring resonator by a simple GaAs tube with inner diameter $D=4.3$ μm, tube wall thickness $t=130$ nm, and tube length $L=10$ μm. Figure 1(a) shows the geometry of the calculated structure. The tube is fixed at planes $P1$ and $P2$ and we assume isotropic GaAs material parameters. The point force F lies in the pressing plane $P3$ and is always applied in a radial direction at the outer tube wall surface. The pressing angle θ_P represents the azimuthal coordinate of F, e.g., $\theta_P=-10°$ corresponds to a force applied in a radial direction above QD2 while $\theta_P=20°$ corresponds to a force applied in a radial direction above QD1 [cf. inset of Fig. 1(b)]. The situation shown in Fig. 1(a) and in the cross section given in the inset of Fig. 1(b) corresponds to $\theta_P=0°$ with an applied force F of 100 μN. The most prominent feature is a considerable displacement of the tube wall inward at the pressing position (red region) and outward in the two regions approximately $\pm 60°$ away from the pressing position [light blue on both sides of the tube—only one is visible in the

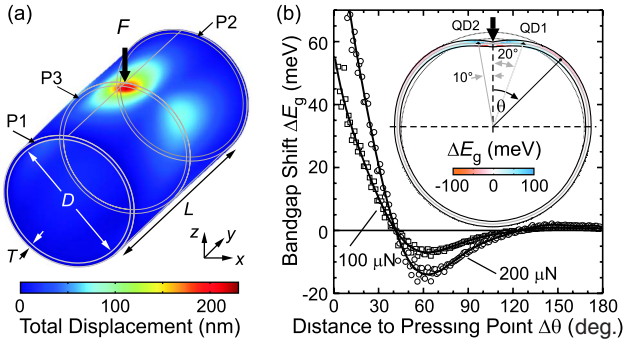

FIG. 1. (Color online) (a) 3D schematic and profile of the total displacement induced by a pressing force F. (b) Calculated band-gap shift ΔE_g as a function of the azimuthal distance from the pressing position ($\Delta\theta=\theta-\theta_P$) for a force strength of 100 μN (open square) and 200 μN (open circle). The solid lines are guides to the eye. The inset shows the profile of the band-gap shift in the pressing plane $P3$ [cf. (a)] for the pressing angle $\theta_P=0$. The positions of QD1 and QD2 correspond to the example discussed in the theory section.

three-dimensional (3D) view]. From the displacement we can derive all strain components induced by the pressing. The strain components in Cartesian coordinates are transformed into polar coordinates and are used to calculate the energy band-gap shift ΔE_g by applying linear deformation-potential theory.[19,20] Due to the fact that during pressing the strain in the tube resonator changes on a large scale compared to the dimensions of a quantum dot, we do not expect considerable changes in the quantum dot shape, size, and strain profile, and therefore neglect energy shifts connected with these parameters. The two curves in Fig. 1(b) illustrate the local dependence of the band-gap shift ΔE_g in the pressing plane $P3$ for two different strengths of the applied force (squares $F=100$ μN, circles $F=200$ μN). We clearly see that depending on the azimuthal distance from the pressing position ($\Delta\theta=\theta-\theta_P$), *both* upward (blueshift) and downward (redshift) shifts in the range of several tens of millielectron volt are created at the same time for the GaAs band gap. It is noteworthy that small blueshifts are induced by this pressing even at positions far from the pressing position ($\Delta\theta>130°$). A false color profile illustration of the locally varying band-gap shift ΔE_g induced in the pressing plane $P3$ by a force of 100 μN is given in the inset of Fig. 1(b).

In order to illustrate the possibility of tuning two QD transition energies into resonance with a resonator mode, we first focus on one specific example:

(i) QD1 and QD2 are located in the pressing plane $P3$.

(ii) The azimuthal coordinate is $\theta=20°$ for QD1 and $\theta=-10°$ for QD2 [cf. inset of Fig. 1(b)]. Both QDs are located in the middle of the tube wall.

(iii) QD1 is assumed to emit at 925 nm ($E_{\mathrm{QD1}}=1.3405$ eV). QD2 is assumed to emit at 910 nm ($E_{\mathrm{QD2}}=1.3626$ eV).

(iv) The optical mode emission line of the microtube resonator is located in between at 914.5 nm (1.3560 eV).

(v) The mode line does not shift when a force is applied to the tube. Pressing experiments show that shifts due to a change in the resonator shape or due to strain induced changes in refractive index are small and can be neglected.

(vi) Tilting of the energy-band edges due to the radial strain gradient and a change in quantization effects due to the pressing are neglected.

Figure 2(a) illustrates the emission energy of QD1 (red lines) and QD2 (blue lines) for three different pressing angles as a function of the pressing force F. For all pressing angles, we find a force strength which leads to a resonance of QD1 and QD2 (intersection of the lines marked with a circle/star and θ_P). In general, resonance is only possible within a certain energy range $\{E_{\mathrm{low}},E_{\mathrm{high}}\}$, which corresponds to a certain set of pairs (F,θ_P). As shown in Fig. 2(b), the spectral position of the resonance between QD1 and QD2 is a continuous function of the pressing angle within this energy range. This means that QD1 and QD2 can be brought into resonance at any energy within this energy range, or in other words, it is possible to bring QD1 and QD2 into resonance with any resonator mode line within this energy range. Interestingly, the width of the energy range $\Delta E_{\mathrm{range}}=E_{\mathrm{high}}-E_{\mathrm{low}}\approx 47$ meV shown in Fig. 2(b), which is derived for moderate force strengths of up to $F=200$ μN [cf. Fig. 2(c)] is two times larger than the typical distance between two resonator

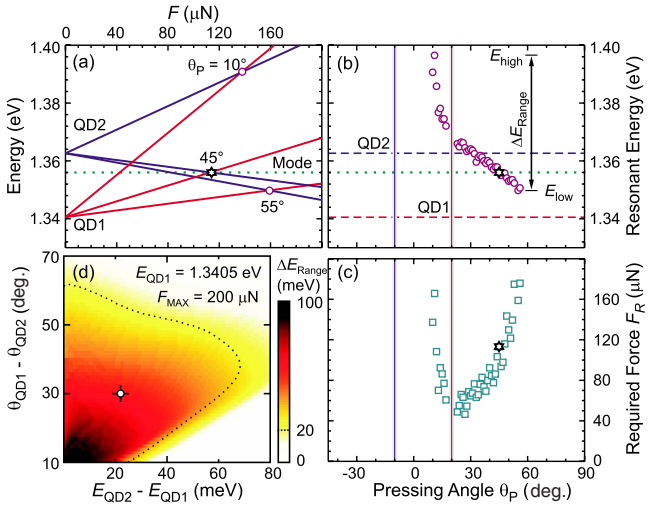

FIG. 2. (Color online) The stars in (a), (b), and (c) indicate the same QD-QD-mode resonance. (a) Calculated transition energies of QD1 and QD2 as a function of applied force F. The optical mode energy is presented as a dotted line. Open circles indicate QD-QD resonance. (b) Resonant energies as a function of the pressing angle. Initial transition energies and azimuthal positions of QD1 and QD2 are shown as lines. (c) Force F_R required to bring QD1 and QD2 into resonance at the resonant energies shown in (b). (d) Width of resonant energy range [cf. (b)] as a function of the azimuthal and spectral distance of QD1 and QD2. The dotted line marks the area with $\Delta E_{\mathrm{range}}>\Delta E_{\mathrm{modes}}$ (for detailed explanations, see text).

modes ($\Delta E_{\mathrm{modes}}\approx 20$ meV, cf. experimental part). Therefore, there is always at least one mode line reachable for a resonance with QD1 and QD2. For the mode line energy assumed in this example [dotted line in Figs. 2(a) and 2(b)], we obtain resonance with QD1 and QD2 for $\theta_P=45°$ and $F=113$ μN. This resonance is marked by the stars in Figs. 2(a)–2(c).

Finally, we consider the case where emission and location of QD2 is varied while QD1 is fixed at 1.3405 eV and $\theta=20°$. The false color plot in Fig. 2(d) shows the width of the resonant energy range as a function of the spectral and local (azimuthal) distances of QD1 and QD2. In the white area, the QDs are spectrally and locally far apart and no resonance is possible. For QDs both spectrally and spatially closer together, large resonant energy ranges of up to approximately 100 meV are possible (dark area). The dotted line marks the area with $\Delta E_{\mathrm{range}}>\Delta E_{\mathrm{modes}}$, i.e., in this area resonance of QD1, QD2, and a resonator mode is always possible. Most situations in an experiment are likely to occur in this area, which underlines the relevance of our approach. The example discussed above [conditions (i)–(vi)] is marked by the white dot in Fig. 2(d).

To experimentally verify the feasibility of the above tuning concept, we proceed as follows: The flexible tube resonators are fabricated by rolling up strained semiconductor bilayers grown by molecular beam epitaxy (MBE).[21,22] Recently, whispering gallery modelike resonances in such structures could be demonstrated by using high-density self-assembled QDs (Refs. 13 and 15) or high-density silicon nanoclusters[16] as inner light sources. Here we introduce the

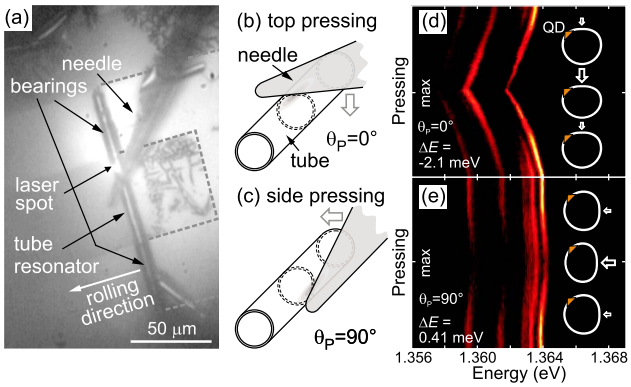

FIG. 3. (Color online) (a) Optical microscopy insight into the cryostat: A rolled up microtube resonator with a glass needle used for *in situ* pressing. (b) and (c) Schematic of the resonator and the glass needle for top- ($\theta_P \approx 0°$) and side- ($\theta_P \approx 90°$) pressing. (d) and (e) Evolution of the PL from a single QD during pressing for $\theta_P \approx 0°$ and $\theta_P \approx 90°$. The inset shows a cross-sectional schematic of the deformed tube. The triangle indicates the azimuthal position of the QD.

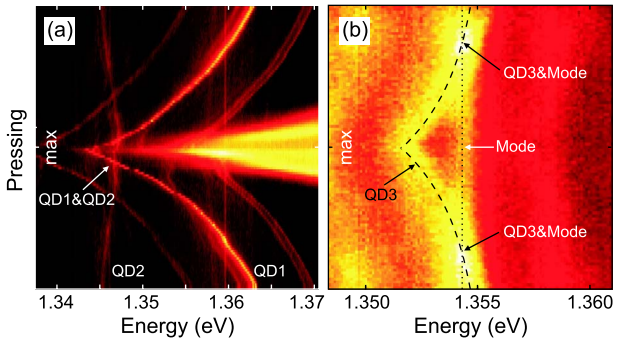

FIG. 4. (Color online) (a) Evolution of PL from two QDs during pressing with $\theta_P \approx 0°$. As indicated by the arrow, resonance of QD1 and QD2 occurs at 1.3472 eV. (b) PL of a single QD and a resonator mode. The mode (dotted line) is almost independent of the applied pressing force and is crossed two times by the QD line (QD3, dashed line) which reversibly shifts with the applied force.

possibility to perform single QD spectroscopy in rolled up microtube resonators by embedding In(Ga)As QDs with low density into the resonator walls. For that purpose, we used the following MBE-layer sequence: 400 nm GaAs buffer layer, 20 nm AlAs sacrificial layer, 15 nm $In_{17}Al_{20}Ga_{63}As$ strained layer, 15 nm GaAs, nominal 1.7 ML InAs, and 25 nm GaAs capping layer. An *in situ* partial capping and annealing step[28] was used to tune the initial emission wavelength of the QDs into the sensitivity range of the Si detector used in the photoluminescence measurements described below. After MBE growth, the wafer is exposed to a three step lithographic procedure to obtain arrays of suspended microtube resonators. Step (1): Definition of *U*-shaped strained mesa. Step (2): Definition of starting edges. Step (3): Rolling up of the strained layers by selectively etching the AlAs layer with hydrofluoric acid. More details of the procedure can be found in Ref. 13. An optical microscope image of a typical microtube resonator is shown in Fig. 3(a). The resonator was rolled up from the *U*-shaped area bordered by the dotted line. The suspended state of the resonator, obtained by the higher number of rotations in the bearings, is necessary to avoid leakage of the modes into the GaAs substrate.

After preparation, the sample is mounted in a cold-finger helium flow cryostat which can be moved by computer controlled *xy*-linear translation stages for exact positioning with a spatial resolution of 50 nm. Microphotoluminescence (μ-PL) measurements are performed at $T=8$ K using a frequency-doubled Nd:YVO_4 laser operating at 532 nm. The laser is focused by a microscope objective (with numerical aperture NA=0.42) to a spot diameter of 1.5 μm. The same microscope objective is used to collect the PL emission. The collected luminescence is then analyzed by a spectrometer equipped with a liquid nitrogen cooled charge coupled device. To *in situ* apply forces to the tube resonators while recording the change in PL, we employ a glass needle mounted on a *x*-*y*-*z* piezotranslation stage (attocube systems). Except for quantum dots in the direct vicinity of the pressing point, the finite-sized glass needle well resembles the point force used in our calculations.

After selecting an adequate resonator, we focus on the QD or pair of QDs to be investigated and position the glass needle next to the laser spot. The orientation of the glass needle relative to the microtube resonator is illustrated in Figs. 3(a)–3(c). Pressing on top of the tube [cf. Fig. 3(b)] corresponds to $\theta_P \approx 0°$ and pressing from the side [cf. Fig. 3(c)] corresponds to $\theta_P \approx 90°$. These two pressing angles are used in our experiment to record the PL as a function of the pressing force.

First we demonstrate the bi-directional tuning of a QD: Figures 3(d) and 3(e) show the evolution of the PL of a single QD in a tube resonator during pressing. We did not attempt to quantify the actual force applied to the tube. The insets illustrate the estimated tube deformation corresponding to $\theta_P \approx 0°$ and $\theta_P \approx 90°$. The diameter and the tube wall thickness of the rolled-up tube resonators correspond to the values used in the above calculations ($D=4.3$ μm, 55 nm strained mesa rolled up in 2.3 rotations result in $t \approx 130$ nm overall tube wall thickness). As predicted, both reversible blueshift and redshift of the whole emission spectrum are observed. As the focus of the objective lens of the μ-PL setup is optimized on the QD before pressing, we slightly loose excitation intensity and collection efficiency during pressing. This effect can be turned around by optimizing the focus on the QD when the resonator is pressed (not shown). For $\theta_P \approx 0°$ [Fig. 3(d)], the QD spectrum redshifts by 2.1 meV and turns back to the initial position as soon as the force is released. For $\theta_P \approx 90°$ [Fig. 3(e)], we find a reversible blueshift of 0.41 meV. From the spectral shifts, we estimate the azimuthal position of the QD to be at $\theta \sim -45°$ [see insets of Fig. 3(d) and 3(e)]. This value agrees well with the laser spot position optimized for the QD [cf. Fig. 3(a)].

Figure 4(a) shows the simultaneous bidirectional tuning of two different QDs. In this case, the collection is optimized for the emission of QD1 and the pressing angle is $\theta_P \approx 0°$. Two groups of lines, which shift differently, can be attributed to the emission of QD1 and QD2, respectively. A crossing of two lines is obtained at 1.3472 eV (see arrow), which

indicates spectral resonance of the two QDs. In this case, QD1 shows a large redshift of ~20 meV, while QD2 shows a blueshift of ~3 meV. Interestingly, the spectral lines of QD1 change their relative distance during the pressing process. This cannot be understood within our model, which considers only the bulk band-gap shift. It might rather be explained by a change of the QD wave functions shape induced by anisotropic stress.[23] After releasing the pressing force, the spectrum returns to the initial state. It is noteworthy that the θ-dependent strain state of the deformed tubes [cf. Fig. 1(b)] also causes a splitting of the InAlGaAs related emission line, which occurs as soon as the tubes are deformed (not shown).

Finally, Fig. 4(b) illustrates the resonance of a single QD with a tube resonator mode. The mode line spacings in our resonators are typically on the order of 20 meV. The quality factor ranges between 1000 and 4000. QD3 (dashed line) can easily be tuned in and out of resonance with the mode (dotted line) by changing the applied force strength (pressing angle $\theta_P \approx 0°$). The resonance occurs at 1.3545 eV. While the QD shows a redshift of ~2.5 meV, the optical mode remains constant within 0.2 meV.

In conclusion, local stress is a promising tool to apply energy shifts to individual close-by QDs in a deterministic fashion. As an example, two QDs in a ring resonator might be tuned into a mode mediated resonance. By means of FEM simulations, we predict that spectral coincidence can be achieved if the QDs are distributed on a ring in a flexible tube resonator. Deforming this tube resonator in an adequate way can be used to induce QD-QD, QD-mode, or QD-QD-mode resonances. First experiments demonstrate spectral shifts of up to 20 meV, bidirectional tuning of a single QD, simultaneous bidirectional tuning of two QDs, as well as spectral coincidence between two QDs and between a single QD and a resonator mode. In view of future quantum electrodynamics experiments,[7,8,24,25] our technique to achieve spectral coincidence might be combined with existing techniques for spatial coincidence.[26,27]

This work was financially supported by BMBF (Contract No. 03N8711) and the DFG (Contract No. Schm1298/5-1).

*Corresponding author. Present address: Institute for Applied Physics, Jungiusstraße 11, 20355 Hamburg, Germany. smendach@physnet.uni-hamburg.de

†Present address: Institute for Integrative Nanosciences, IFW Dresden, Helmholtzstraße 20, 01069 Dresden, Germany.

‡Present address: CEA-LETI, MINATEC, 17 rue des Martyrs, 38054-Grenoble, France

[1] A. J. Shields, Nat. Photonics **1**, 215 (2007).
[2] I. Fushman, D. Englund, A. Faraon, N. Stoltz, P. Petroff, and J. Vuckovic, Science **320**, 769 (2008).
[3] L. Robledo, J. Elzerman, G. Jundt, M. Atatüre, A. Högele, S. Fält, and A. Imamoglu, Science **320**, 772 (2008).
[4] S. Fafard and C. N. Allen, Appl. Phys. Lett. **75**, 2374 (1999).
[5] A. Rastelli, A. Ulhaq, S. Kiravittaya, L. Wang, A. Zrenner, and O. G. Schmidt, Appl. Phys. Lett. **90**, 073120 (2007).
[6] A. Babinski, G. Ortner, S. Raymond, M. Potemski, M. Bayer, W. Sheng, P. Hawrylak, Z. Wasilewski, S. Faradand A. Forchel, Phys. Rev. B **74**, 075310 (2006).
[7] J. P. Reithmaier, G. Sęk, A. Löffler, C. Hofmann, S. Kuhn, S. Reitzenstein, L. V. Keldysh, V. D. Kulakovskii, T. L. Reinecke, and A. Forchel, Nature (London) **432**, 197 (2004).
[8] T. Yoshie, A. Scherer, J. Hendrickson, G. Khitrova, H. M. Gibbs, G. Rupper, C. Ell, O. B. Shchekin, and D. G. Deppe, Nature (London) **432**, 200 (2004).
[9] S. Seidl, M. Kroner, A. Högele, K. Karrai, R. J. Warburton, A. Badolato, and P. M. Petroff, Appl. Phys. Lett. **88**, 203113 (2006).
[10] A. Imamoğlu, S. Fält, J. Dreiser, G. Fernandez, M. Atatüre, K. Hennessy, A. Badolato, and D. Gerace, J. Appl. Phys. **101**, 081602 (2007).
[11] H. J. Krenner, E. C. Clark, T. Nakaoka, M. Bichler, C. Scheurer, G. Abstreiter, and J. J. Finley, Phys. Rev. Lett. **97**, 076403 (2006).
[12] S. Mendach, H. Welsch, O. Schumacher, Ch. Heyn, and W. Hansen, Semicond. Sci. Technol. **20**, 402 (2005).
[13] T. Kipp, H. Welsch, Ch. Strelow, Ch. Heyn, and D. Heitmann, Phys. Rev. Lett. **96**, 077403 (2006).
[14] S. Mendach, R. Songmuang, S. Kiravittaya, A. Rastelli, M. Benyoucef, and O. G. Schmidt, Appl. Phys. Lett. **88**, 111120 (2006).
[15] S. Mendach, R. Songmuang, M. Benyoucef, A. Rastelli, and O. G. Schmidt, AIP Conf. Proc. **893**, 1149 (2007).
[16] R. Songmuang, A. Rastelli, S. Mendach, and O. G. Schmidt, Appl. Phys. Lett. **90**, 091905 (2007).
[17] Ch. Strelow, C. M. Schultz, H. Rehberg, H. Welsch, Ch. Heyn, D. Heitmann, and T. Kipp, Phys. Rev. B **76**, 045303 (2007).
[18] Structural mechanics module with COMSOL MULTIPHYSICS software package is used and linear elasticity is assumed throughout this study. (See www.femlab.de for more details).
[19] C. G. Van de Walle, Phys. Rev. B **39**, 1871 (1989).
[20] E. P. O'Reilly, Semicond. Sci. Technol. **4**, 121 (1989).
[21] V. Ya. Prinz, V. A. Seleznev, A. K. Gutakovsky, A. V. Chehovskiy, V. V. Preobrazhenskii, M. A. Putyato, and T. A. Gavrilova, Physica E (Amsterdam) **6**, 828 (2000).
[22] O. G. Schmidt and K. Eberl, Nature (London) **410**, 168 (2001).
[23] O. Stier, M. Grundmann, and D. Bimberg, Phys. Rev. B **59**, 5688 (1999).
[24] E. Peter, P. Senellart, D. Martrou, A. Lemaitre, J. Hours, J. M. Gerard, and J. Bloch, Phys. Rev. Lett. **95**, 067401 (2005).
[25] K. Hennessy, A. Badolato, M. Winger, D. Gerace, M. Atatüre, S. Gulde, S. Fält, E. L. Hu, and A. Imamoğlu, Nature (London) **445**, 896 (2007).
[26] *Lateral Alignment of Epitaxial Quantum Dots*, edited by O. G. Schmidt (Springer, Berlin, 2007).
[27] S. Kiravittaya, M. Benyoucef, R. Zapf–Gottwick, A. Rastelli, and O. G. Schmidt, Appl. Phys. Lett. **89**, 233102 (2006).
[28] Z. R. Wasilewski, S. Fafard, and J. P. McCaffrey, J. Cryst. Growth **201-202**, 1131 (1999).